Absorption of light by soot particles in micro-droplets of water

Vadim A. Markel*

Department of Physics and Astronomy, University of Georgia, Athens, GA 30602

Vladimir M. Shalaev[†]

Department of Physics, New Mexico State University, Las Cruces, NM 88003

Absorption cross section of carbon soot clusters inside water microdroplets is calculated. Fractal geometry of carbon inclusions is considered with the fractal dimension D in the interval $1 \leq D \leq 3$, which includes the trivial geometry ($D = 3$) as a limiting case. It is found that the absorption cross section of a soot cluster inside a water droplet is increased, compared to that in vacuum, by the factor of ≈ 16 for the practically important case of $D = 1.8$. This result is obtained by averaging of the enhancement factor over the diffraction parameter of the microdroplets $x = ka$ ($k = 2\pi/\lambda$, a - radius of the microdroplet) with a fine resolution. It is shown that the narrow resonances in the enhancement factor as a function of x play important role and should be taken into account for the purpose of averaging over x. The absorption enhancement factor increases, on average, when D decreases, and reaches the value of ≈ 22 for $D = 1$.

Key words: microdroplets, fractal clusters, carbon soot, absorption

1. Introduction

The effects of radiation absorbing carbonaceous atmospheric pollutants on the global climate and radiation energy transfer attracted much attention recently[1-4]. It is, generally, believed that such pollutants act oppositely to the green house effect (for the "nuclear winter" effect, see, for example, Ref. 5). While this general tendency is more or less obvious, obtaining reliable quantitative results is complicated by the following two factors. First, small carbon particles that form in the process of incomplete combustion of carbohydrates, typically, aggregate and stick to each other to form large random clusters with complex fractal morphology[6-11]. The second important factor is that these soot clusters often form agglomerates with water microdroplets, especially in the clouds[1,12-15]. The goal of this paper is to obtain quantitative results for absorption characteristics of such composite microdroplets with account of the fractal morphology of carbon soot clusters. Our consideration includes the non-fractal homogeneous distribution of carbon inclusions as the limiting case.

Foundations of the theory of scattering and absorption of plain electromagnetic waves by fractal smoke clusters were built by Berry and Percival[16] and Martin and Hurd[17]. The theory was developed in many detail in the past few years[10,11,18-25]. In these papers, scattering is considered either in the first Born approximation[17], or in the mean-field approximation[16]. The main physical assumption leading to applicability of the first Born approximation is that the frequency of the incident wave is far from any of the collective dipole resonances of the scattering system. This assumption is accurate for scattering of visible light by clusters built from black carbon particles. In the mean-field approximation, one assumes that all the collective dipole resonances are degenerate (have the same frequency), while the frequency of the incident wave can be arbitrary. Mathematically, these approximations are similar (in fact, they give the same expression for the scattering amplitude, differing by a multiplicative factor). It is important that in both approximations the incident electromagnetic field is given by a plane wave and is not coupled to the scattered waves.

When a cluster is placed inside a water droplet, it is no longer exited by a plane wave, but rather by internal modes of a high-quality optical resonator. To complicate things further, the resonator modes can effectively couple to the modes of clusters themselves. There have been a considerable number of experimental[26-31] and theoretical[32-40] studies of scattering and absorbing properties of inhomogeneous spheres carried out. Below, we briefly review the theoretical approaches to the problem.

The simplest model for a water droplet with an inclusion inside is a spherical dielectric particle with an eccentric spherical inclusion. An exact formal solution to the problem of light scattering and absorption by such composite spheres was obtained by Borghese *et al.*[33] and generalized for the case of multiple arbitrarily positioned spherical inclusions by Borghese *et al.*[36] and Fuller[37,38,41,42] The solutions were obtained by the vector spherical harmonic (VSH) expansion of electrical fields inside the homogeneous spherical regions and satisfying the boundary conditions at all the discontinuity surfaces. Even in the case of one spherical inclusion, the solution must be obtained from a system of linear equations that is, theoretically, infinite-order. Practically, the VSH expansion is truncated at some maximum order, L, and then the system contains $\sim L^2$ equations[33]. When multiple inclusions are considered, the number of equations is further increased, which makes the problem very complicated numerically. Also, the approach based on the exact boundary conditions consideration requires knowledge of the exact geometry of the problem before the time-extensive calculations. This fact complicates averaging of solutions over random distribution of inclusions inside water droplets.

An alternative approach based on the perturbation theory was developed by Kerker *et al.*[32] and Hill *et al.*[39]. According to this method, the dielectric function of an inhomogeneous sphere is represented as a sum of a constant (unperturbed) value and a small coordinate-dependent perturbation. In the zero approximation, the field inside the droplet is calculated in the assumption that the perturbation of the dielectric function is equal to zero. This field is given by the Mie expansion in terms of the VSH. In the next iteration, the zero-approximation field induces some additional polarization (or, equivalently, current) in the volume, proportional to the perturbation of the dielectric function. This additional polarization can be used to calculate changes of scattering and absorbing characteristics of the inhomogeneous sphere as compared to the homogeneous (unperturbed) one. A big advantage of this method is that it allows one to perform averaging over random perturbations. However, it has a drawback. As was pointed out by Hill *et al.*[39], the internal field must be computed iteratively. That is, the additional polarization calculated in the first iteration described above should produce some additional internal electrical field, which, in turn, gives rise to additional polarization (now proportional to the unperturbed dielectric function), and so on. Physically, this means that the modes of a homogeneous spherical resonator are coupled to the modes of the inhomogeneous perturbation of

the dielectric function. In order for a finite-order approximation to be accurate, it is necessary that the perturbation expansion of any physical quantity under consideration converges. In section 2 B we show that, in general, it is not the case. More specifically, this expansion always diverges for physical quantities related to scattering (such as the differential scattering cross section). However, the perturbation expansion converges for the absorption cross-section when the imaginary part of the unperturbed dielectric function is zero (or sufficiently small).

In this paper, we use the above fact to calculate absorption cross sections of carbon smoke particles inside spherical water droplets in the first order of the perturbation theory. The perturbation expansion is mathematically similar to that of Kerker *et al.*[32] and Hill *et al.*[39]. The water itself is assumed to be non-absorbing. We perform calculations for fractal distribution of carbon inclusions with a power-law dependence of density on the distance from the center of a water droplet; the case of trivial (non-fractal) geometry is considered as a limiting case when $D = 3$. We calculate enhancement factor for the absorption cross sections of carbon smoke inside a water droplet as compared to that of free carbon smoke. We show that the absorption enhancement factor shows little systematic dependence on the diffraction parameter of the host sphere $x = 2\pi/\lambda$, apart from quasi-random resonances which are very narrow. This fact allowed us to average the enhancement factor over x with a fine resolution in x, so that most resonances were resolved. Physically, this averaging corresponds to either a polydisperse ensemble of water droplets or probing by a broad-band radiation. Because of the presence of narrow resonances, our averaged absorption factor turned out to be larger by the factor of $\sim 4-5$ than that calculated for a randomly selected value of x. For the trivial distribution of carbon inclusions ($D = 3$), we obtain the averaged enhancement factor of 14, while for a randomly selected value of x the typical (most probable) enhancement factor is from 2 to 4. This suggests that, although the resonances in x are very narrow, they are not small in the integral sense, and should be taken into account.

The averaging procedure involved in our calculations might explain why our estimates of the enhancement factor are significantly larger than those reported earlier[4,41−43]. Fuller calculated the specific absorption cross section for a single spherical carbon grain located near the surface of a water droplet[41] and inside the water droplet[42] as a function of the grain's position. Although Fuller's data are not averaged over the whole volume of the microdroplet, they indicate that the volume-averaged absorption enhancement factor is smaller than 14. Chylek *et al.* averaged the same quantity for the carbon inclusion location distributed evenly within a spherical cone with the axis collinear to the incident wave propagation direction[4] and over the whole volume[43]. In the first case the authors estimate[44] the enhancement factor to be ≈ 4, and in the second ≈ 2. However all of the above calculations were performed for a fixed value of the diffraction parameter x. Because the resonances are very narrow, it is unlikely that a randomly selected value of x will lie within a resonance. Our calculations indicate that if x is chosen exactly in resonance, the volume-averaged enhancement factor can be as large as 10^4.

The approach developed in this paper applies to any spherical highly transparent microcavities doped with strongly absorbing inclusions with the fractal dimension from 1 to 3, not just to carbon soot inside water droplets. However, the numerical results are strongly dependent on the refractive index of the host. The difference between microdroplets with refractive index of water (~ 1.33) and of sulfate (~ 1.52) was demonstrated by Fuller[41,42].

In section 2 we review the general formulation of the scattering problem, integral equation formalism and the perturbation expansion. In this section we also introduce definition for the absorption enhancement factor. In section 3 we take account of the fact that any density distribution of inclusions inside a spherical volume must be spherically symmetrical on average (provided there is no selected direction) and perform averaging over spatial angles. In section 4 we consider the fractal geometry of carbon inclusions and corresponding radial integrals. In section 5 we present results of numerical calculations of the absorption enhancement factor for different fractal dimensions. Lastly, section 6 contains a summary.

2. Basic theory

A. Formulation of the model

Consider a plane monochromatic wave of the form

$$\mathbf{E}_{inc}(\mathbf{r}, t) = \mathbf{E}_0 \exp(i\mathbf{k} \cdot \mathbf{r} - \omega t) \tag{1}$$

incident on a spherical water droplet of a radius a containing a carbon soot cluster inside. The time dependence, $\exp(-i\omega t)$, is the same for all time-varying fields and, therefore, will be omitted below.

The physical system under consideration can be characterized by a dielectric function of the form

$$\epsilon(\mathbf{r}) = \begin{cases} \epsilon_1 + (\epsilon_2 - \epsilon_1)\rho(\mathbf{r}) \ , & r \leq a \\ 1, & r > a \end{cases} .$$

(2)

Here ϵ_1 and ϵ_2 are the dielectric constants of water and carbon, respectively, and $\rho(\mathbf{r})$ is the density of carbon inclusions inside the droplet, normalized by the condition

$$\int_V \rho(\mathbf{r}) d^3\mathbf{r} = v \ ,$$

(3)

where v is the total volume occupied by carbon and $V = 4\pi a^3/3$ is the volume of the droplet; $\int_V$ denotes integration over the spatial area defined by $r \leq a$ ($\int_V d^3\mathbf{r} = V$). We assume that the volume fraction of carbon is small, so that the small parameter of the problem is v/V. We also assume that $\rho(\mathbf{r}) = 0$ for $r > a$, i.e. the soot cluster is completely covered by water.

In our notations, $\rho(\mathbf{r})$ denotes the exact density of carbon inclusions for some given random realization of a soot cluster. As such, $\rho(\mathbf{r}) = 1$ if the radius-vector $\mathbf{r}$ lies in the area occupied by carbon, and $\rho(\mathbf{r}) = 0$ otherwise. We will see that for calculation of some average physical characteristics, such as absorption, one needs to average $\rho(\mathbf{r})$ over random realizations of carbon soot clusters. We denote the average density by $\langle\rho(\mathbf{r})\rangle$; it can be interpreted as the probability to find some given point $\mathbf{r}$ inside a droplet occupied by carbon. If $\langle\rho(\mathbf{r})\rangle$ is bounded everywhere inside the sphere, the condition $v/V \ll 1$ implies that $\langle\rho(\mathbf{r})\rangle \ll 1 \ \forall \ \mathbf{r}$.

B. Integral equations formalism

The vector wave equation for the monochromatic electrical field $\mathbf{E}(\mathbf{r})$ reads

$$\left[\nabla^2 + k^2\epsilon(\mathbf{r})\right]\mathbf{E}(\mathbf{r}) = 0 \ ; \quad \nabla \cdot \mathbf{E}(\mathbf{r}) = 0 \ ,$$

(4)

where $k = \omega/c$ is the wave vector in the free space and $\epsilon(\mathbf{r})$ is the dielectric function (at the given frequency ω), defined by formula (2).

Using the free-space dyadic Green's function $\hat{G}(\mathbf{r})$ for the vector wave equation, we can rewrite (4) in the integral form:

$$\mathbf{E}(\mathbf{r}) = \mathbf{E}_{inc}(\mathbf{r}) + \int_V \hat{G}(\mathbf{r} - \mathbf{r}')\frac{\epsilon(\mathbf{r}') - 1}{4\pi}\mathbf{E}(\mathbf{r}')d^3\mathbf{r}' \ .$$

(5)

The Green's function, $\hat{G}$, is given by general formulas for dipole radiation of a point source (for derivation of the Green's function, see Ref. 45, Chapter 9 or Ref. 46 , Chapter 6; an explicit coordinate system-independent expression for the regular part of the Green's function is given, for example, by Markel[47]). For our analysis, we do not need to specify $\hat{G}$ here.

The free term in the right hand side of Eq. (5) was chosen to satisfy the boundary conditions at the infinity, and the integral was extended only over the volume occupied by the droplet, because $\epsilon(\mathbf{r}) = 1$ outside. The radius vector $\mathbf{r}$ can, in principle, lie both inside and outside the sphere. However, all the physically measurable quantities, such as absorption and scattering cross sections, are completely defined by the polarization function which is zero in vacuum. Therefore, it is generally sufficient to restrict our consideration to the class of functions $\mathbf{E}(\mathbf{r})$ defined inside the spherical volume $r < a$, while the boundary conditions are satisfied automatically due to the proper choice of the free term in (5).

At the next step, we represent the electrical field inside the sphere as a sum of two contributions:

$$\mathbf{E}(\mathbf{r}) = \mathbf{E}_s(\mathbf{r}) + \mathbf{E}_c(\mathbf{r}) \ ,$$

(6)

where $\mathbf{E}_s(\mathbf{r})$ is the solution to the equation (5) with $\epsilon_2 = \epsilon_1$, i.e.,

$$\mathbf{E}_s(\mathbf{r}) = \mathbf{E}_{inc}(\mathbf{r}) + \frac{\epsilon_1 - 1}{4\pi}\int_V \hat{G}(\mathbf{r} - \mathbf{r}')\mathbf{E}_s(\mathbf{r}')d^3\mathbf{r}' \ ,$$

(7)

4

and $\mathbf{E}_c(\mathbf{r})$ is the additional term which originates because of the presence of a carbon cluster. $\mathbf{E}_s(\mathbf{r})$ is given by the Mie solution for a dielectric sphere and we assume that it is known. Substituting $\mathbf{E}(\mathbf{r})$ in the form (6) into (5), we find the equation for $\mathbf{E}_c(\mathbf{r})$:

$$\mathbf{E}_c(\mathbf{r}) = \frac{\epsilon_2 - \epsilon_1}{4\pi} \int_V \rho(\mathbf{r}')\hat{G}(\mathbf{r} - \mathbf{r}')\mathbf{E}_s(\mathbf{r}')d^3\mathbf{r}' + \int_V \frac{\epsilon_1 - 1 + (\epsilon_2 - \epsilon_1)\rho(\mathbf{r}')}{4\pi}\hat{G}(\mathbf{r} - \mathbf{r}')\mathbf{E}_c(\mathbf{r}')d^3\mathbf{r}' \ . \tag{8}$$

The first term in (8) with the known function $\mathbf{E}_s(\mathbf{r})$ serves as a free term for the integral equation (8).

For many practical problems knowledge of the ensemble-averaged internal field is sufficient. (Evidently, this class of problems does not include the problems of nonlinear optics that require consideration of fluctuations of the local field.) We cannot perform direct averaging of equation (8) over random realization of inclusions, because such averaging would add an additional unknown term $\langle \rho(\mathbf{r})\mathbf{E}_c(\mathbf{r})\rangle$. In the general case, we cannot factorize this correlator as $\langle \rho(\mathbf{r})\mathbf{E}_c(\mathbf{r})\rangle = \langle \rho(\mathbf{r})\rangle\langle\mathbf{E}_c(\mathbf{r})\rangle$. However, in the linear (in v/V) approximation we can neglect the above term as a higher-order correction. Then it becomes possible to write an equation for the ensemble-average value $\langle\mathbf{E}_c(\mathbf{r})\rangle$:

$$\langle\mathbf{E}_c(\mathbf{r})\rangle = \frac{\epsilon_2 - \epsilon_1}{4\pi} \int_V \langle\rho(\mathbf{r}')\rangle\hat{G}(\mathbf{r} - \mathbf{r}')\mathbf{E}_s(\mathbf{r}')d^3\mathbf{r}' + \frac{\epsilon_1 - 1}{4\pi} \int_V \hat{G}(\mathbf{r} - \mathbf{r}')\langle\mathbf{E}_c(\mathbf{r}')\rangle d^3\mathbf{r}' \ . \tag{9}$$

We can make two important conclusions from the general form of (9). First, the ratio of $|\langle\mathbf{E}_c\rangle|/|\mathbf{E}_s|$ is of the same order of magnitude as v/V. This can be seen by multiplying $\langle\rho(\mathbf{r}')\rangle$ in (9) by some arbitrary constant α. The average field $\langle\mathbf{E}_c(\mathbf{r})\rangle$ is also multiplied by the same factor α. This means, that, on average, $|\langle\mathbf{E}_c(\mathbf{r})\rangle|/|\mathbf{E}_s(\mathbf{r})| \sim \langle\rho(\mathbf{r})\rangle \sim v/V$. A similar result is readily obtained for the exact field $\mathbf{E}_c(\mathbf{r})$ (before the averaging).

The second conclusion is that it is, generally, impossible to apply the Born expansion or similar perturbation expansion for calculation of $\langle\mathbf{E}_c(\mathbf{r})\rangle$. Indeed, both terms in the right-hand side of (9) are of the same order of magnitude (proportional to v/V). Suppose, we start from the zero-order approximation $\langle\mathbf{E}_c^{(0)}(\mathbf{r})\rangle = 0$, and substitute it into (9) to obtain the first order approximation, and so on. It is easy to see that all the terms in the generated expansion will be of the same order of magnitude in terms of v/V, and, therefore, convergence cannot be reached.

The above fact makes the general scattering problem for a water droplet containing a cluster inside very complicated. Indeed, the only small parameter of the problem, v/V, cannot be used to generate a converging expansion for $\mathbf{E}_c(\mathbf{r})$. However, as we show below, we can use the fact that $|\mathbf{E}_c(\mathbf{r})|/|\mathbf{E}_s(\mathbf{r})| \sim v/V$ to calculate the absorption cross-section when water itself is weakly absorbing.

C. Absorption

The absorption cross-section, σ_a, is completely defined by the polarization function, $\mathbf{P}(\mathbf{r}) = [(\epsilon(\mathbf{r}) - 1)/4\pi]\mathbf{E}(\mathbf{r})$. This is a consequence of the fact that the absorbed energy is equal to the total work of the local field in the material (as opposed to the extinction energy, which is equal to the work of the *external* field). The formula for the absorption cross section in terms of the polarization function can be obtained from the optical theorem and direct integration of the scattering amplitude[47,48]:

$$\sigma_a = \frac{16\pi^2 k}{|\mathbf{E_0}|^2} \int_V \frac{\mathrm{Im}\epsilon(\mathbf{r})}{|\epsilon(\mathbf{r}) - 1|^2} |\mathbf{P}(\mathbf{r})|^2 d^3\mathbf{r} \ = \ \frac{k}{|\mathbf{E_0}|^2} \int_V \mathrm{Im}[\epsilon(\mathbf{r})] |\mathbf{E}(\mathbf{r})|^2 d^3\mathbf{r} \ . \tag{10}$$

Using formulas (2) for $\epsilon(\mathbf{r})$ and (6) for $\mathbf{E}(\mathbf{r})$, we can rewrite the above expression for the absorption cross section as

$$\sigma_a = \frac{k\mathrm{Im}\epsilon_1}{|\mathbf{E_0}|^2} \int_V |\mathbf{E}_s(\mathbf{r})|^2 d^3\mathbf{r} \ + \ \frac{k\mathrm{Im}(\epsilon_2 - \epsilon_1)}{|\mathbf{E_0}|^2} \int_V \rho(\mathbf{r}) |\mathbf{E}_s(\mathbf{r})|^2 d^3\mathbf{r} \ +$$
$$\frac{k\mathrm{Im}\epsilon_1}{|\mathbf{E_0}|^2} \int_V \left\{ 2\mathrm{Re}\left[\mathbf{E}_s(\mathbf{r}) \cdot \mathbf{E}_c^*(\mathbf{r})\right] + |\mathbf{E}_c(\mathbf{r})|^2 \right\} d^3\mathbf{r} \ +$$
$$\frac{k\mathrm{Im}(\epsilon_2 - \epsilon_1)}{|\mathbf{E_0}|^2} \int_V \rho(\mathbf{r}) \left\{ 2\mathrm{Re}\left[\mathbf{E}_s(\mathbf{r}) \cdot \mathbf{E}_c^*(\mathbf{r})\right] + |\mathbf{E}_c(\mathbf{r})|^2 \right\} d^3\mathbf{r} \ . \tag{11}$$

Now we analyze the terms in the right-hand side of (11). The first term gives the absorption cross section by a water droplet without inclusions. It is given by the well-known Mie solution and, consequently, is of no interest for

us. Taking into account that $\langle \rho(\mathbf{r}) \rangle \sim |\mathbf{E}_c|/|\mathbf{E}_s| \sim v/V$, we find that the second and the third terms are of the same order of magnitude and give the first correction of of the order of v/V to the absorption cross sections. Finally, the fourth term is of the order of $(v/V)^2$, and can be neglected in the first approximation.

Even in the first approximation, the expression for the absorption cross section contains the unknown field $\mathbf{E}_c(\mathbf{r})$ in the third term of (11). However, for the particular case of carbon and water, $\mathrm{Im}\epsilon_2 \gg \mathrm{Im}\epsilon_1$. This additional factor allows one to neglect the third term in expansion (11). In principle, the first term can be still large or comparable to the second one due to the large factor V/v, but this fact does not complicate further derivations.

Finally, we can represent the absorption cross section as $\sigma_a = \sigma_{a,water} + \sigma_{a,carbon}$ where $\sigma_{a,water}$ is given by the first term in (11), and

$$\sigma_{a,carbon} = \frac{k\mathrm{Im}\epsilon_2}{|\mathbf{E_0}|^2} \int_V \rho(\mathbf{r}) \, |\mathbf{E}_s(\mathbf{r})|^2 \, d^3\mathbf{r} \ . \tag{12}$$

The above formula gives the absorption cross section associated with carbon inclusions in the first order in v/V; the higher corrections are of the order of $(v/V)^2$. In the ideal case of $\mathrm{Im}\epsilon_1 = 0$, this formula gives the total absorption of a composite droplet. Below, we will assume for simplicity that ϵ_1 is a real number.

Since ρ and $\mathbf{E}_s$ are statistically independent, we can perform direct averaging of (12) over random realizations of carbon soot inclusions:

$$\langle \sigma_{a,carbon} \rangle = \frac{k\mathrm{Im}\epsilon_2}{|\mathbf{E_0}|^2} \int_V \langle \rho(\mathbf{r}) \rangle \, |\mathbf{E}_s(\mathbf{r})|^2 \, d^3\mathbf{r} \ . \tag{13}$$

Note that in the above averaging the radius of a water droplet is fixed.

D. Enhancement factor

We define the enhancement factor G as the ratio of the absorption cross section of a carbon soot cluster in a water micro-droplet, defined by (13) to that in vacuum:

$$G = \frac{\langle \sigma_{a,carbon} \rangle}{\langle \sigma_{a,carbon}^{(0)} \rangle} \ , \tag{14}$$

where $\langle \sigma_{a,carbon}^{(0)} \rangle$ is the average absorption cross section of carbon soot in vacuum. The latter can be easily calculated using equation (10) and replacing $\mathbf{E}(\mathbf{r})$ by $\mathbf{E}_{inc}(\mathbf{r})$. Taking into account that $|\mathbf{E}_{inc}(\mathbf{r})|^2 = |\mathbf{E}_0|^2$ and $\epsilon(\mathbf{r}) = 1 + (\epsilon_2 - 1)\rho(\mathbf{r})$ for carbon soot in vacuum, we find that $\langle \sigma_{a,carbon}^{(0)} \rangle = kv\mathrm{Im}\epsilon_2$ and

$$G = \frac{1}{v|\mathbf{E_0}|^2} \int_V \langle \rho(\mathbf{r}) \rangle \, |\mathbf{E}_s(\mathbf{r})|^2 \, d^3\mathbf{r} \ . \tag{15}$$

3. Angular integration

The average density of carbon inclusions $\langle \rho(\mathbf{r}) \rangle$ must be spherically symmetrical: $\langle \rho(\mathbf{r}) \rangle = \langle \rho(r) \rangle$. Therefore, the angular integration in (15) can be done in the most general form, without specifying $\langle \rho \rangle$:

$$G = \frac{1}{|\mathbf{E_0}|^2 v} \int_0^a r^2 \langle \rho(r) \rangle dr \int |\mathbf{E}_s(\mathbf{r})|^2 \, d\Omega \ . \tag{16}$$

The internal field $\mathbf{E}_s$ is given by the expansion in terms of the VSH's, $\mathbf{M}_{omn}$, $\mathbf{M}_{emn}$, $\mathbf{N}_{omn}$ and $\mathbf{N}_{emn}$ (for a detailed description of the VSH expansion see Ref. 49). For a plane incident wave, only the VSH's with $m = 1$ are left in this expansion. Further, if the incident wave is polarized along the x-axis, $\mathbf{M}_{e1n}$ and $\mathbf{N}_{o1n}$ are not excited.

6

For the linear absorption, it is sufficient to consider a linear polarization of the incident wave. An elliptical polarization can be described as a superposition of two linearly polarized waves; the absorbed power due to these two waves is added up because of the linear nature of the interaction. Below, we will adopt the linear polarization of the incident wave along the x-axis ($\mathbf{E}_0 = \mathbf{e}_x E_0$), and will use the following simplified notations for the VSH's that can be excited in this particular case: $\mathbf{M_n} \equiv \mathbf{M}_{o1n}$ and $\mathbf{N}_n \equiv \mathbf{N}_{e1n}$. Then the expansion for the $\mathbf{E}_s$ field takes the form

$$\mathbf{E}_s = \sum_{n=1}^{\infty} i^n \frac{E_0(2n+1)}{n(n+1)} \left(c_n \mathbf{M}_n - i d_n \mathbf{N}_n\right) \ . \tag{17}$$

Here c_n and d_n are the internal field coefficients[49] defined by

$$c_n = \frac{j_n(x)\left[xh_n^{(1)}(x)\right]' - h_n^{(1)}(x)\left[xj_n(x)\right]'}{j_n(x_1)\left[xh_n^{(1)}(x)\right]' - h_n^{(1)}(x)\left[x_1 j_n(x_1)\right]'} \ ; \tag{18}$$

$$d_n = \frac{j_n(x)\left[xh_n^{(1)}(x)\right]' - h_n^{(1)}(x)\left[xj_n(x)\right]'}{(x_1/x)j_n(x_1)\left[xh_n^{(1)}(x)\right]' - (x/x_1)h_n^{(1)}(x)\left[x_1 j_n(x_1)\right]'} \ ; \tag{19}$$

$$x = ka \ ; \quad x_1 = k_1 a \ ; \quad k_1 = \sqrt{\epsilon_1}k \ , \tag{20}$$

where $j_n(x)$ and $h^{(1)}(x)$ are the spherical Bessel and Hankel functions of the first kind, respectively, and prime denotes differentiation with respect to the argument in parenthesis.

The VSH's are mutually orthogonal in the sense that

$$\int \mathbf{M}_n \cdot \mathbf{M}_m \, d\Omega = 0 \ , \quad \text{if } n \neq m \ ; \tag{21}$$

$$\int \mathbf{N}_n \cdot \mathbf{N}_m \, d\Omega = 0 \ , \quad \text{if } n \neq m \ ; \tag{22}$$

$$\int \mathbf{M}_n \cdot \mathbf{N}_m \, d\Omega = 0 \ , \quad \forall n \text{ and } m \ . \tag{23}$$

Consequently, the angular integral in (16) can be written as

$$\int |\mathbf{E}_s(\mathbf{r})|^2 \, d\Omega = \sum_{n=1}^{\infty} \frac{|E_0|^2 (2n+1)^2}{n^2(n+1)^2} \left[|c_n|^2 \int \mathbf{M}_n^2 d\Omega + |d_n|^2 \int \mathbf{N}_n^2 d\Omega\right] \tag{24}$$

Note that for a purely real dielectric constant ϵ_1 the VSH's are also real (see equations (25) and (26) below); this is why $|\mathbf{M}_n|^2$ and $|\mathbf{N}_n|^2$ were replaced by $\mathbf{M}_n^2$ and $\mathbf{N}_n^2$ in (24).

Expressions for the VSH's are usually written[49] in the spherical coordinate system with z-axis coinciding with the direction of propagation of the incident wave, and x-axis — with the polarization vector, and using the local basis $\mathbf{e}_r, \mathbf{e}_\theta, \mathbf{e}_\phi$. However, such representation is not convenient for the angular integration according to (24) because the basis vectors $\mathbf{e}_r, \mathbf{e}_\theta, \mathbf{e}_\phi$ depend themselves on coordinates. Instead, we adduce below expressions for the VSH's as functions of spherical coordinates (r, θ, ϕ), but spanned by the position-independent Cartesian unit vectors $\mathbf{e}_x, \mathbf{e}_y, \mathbf{e}_z$:

$$\mathbf{M}_n(r, \theta, \phi) = j_n(k_1 r)\Big\{\mathbf{e}_x \left[\cos^2\phi \cos\theta \pi_n(\theta) + \sin^2\phi \tau_n(\theta)\right] +$$
$$\mathbf{e}_y \cos\phi \sin\phi\left[\cos\theta \pi_n(\theta) - \tau_n(\theta)\right] - \mathbf{e}_z \cos\phi \sin\theta \pi_n(\theta)\Big\} \ ; \tag{25}$$

$$\mathbf{N}_n(r,\theta,\phi) =$$

$$\mathbf{e}_x \cos^2\phi \left\{ n(n+1)\frac{j_n(k_1 r)}{k_1 r}\sin^2\theta\pi_n(\theta) + \left[\frac{j_n(k_1 r)}{k_1 r} + j_n'(k_1 r)\right]\left[\cos\theta\tau_n(\theta) + \tan^2\phi\pi_n(\theta)\right]\right\} +$$

$$\mathbf{e}_y \cos\phi\sin\phi \left\{ n(n+1)\frac{j_n(k_1 r)}{k_1 r}\sin^2\theta\pi_n(\theta) + \left[\frac{j_n(k_1 r)}{k_1 r} + j_n'(k_1 r)\right]\left[\cos\theta\tau_n(\theta) - \pi_n(\theta)\right]\right\} +$$

$$\mathbf{e}_z \cos\phi\sin\theta \left\{ n(n+1)\frac{j_n(k_1 r)}{k_1 r}\cos\theta\pi_n(\theta) - \left[\frac{j_n(k_1 r)}{k_1 r} + j_n'(k_1 r)\right]\tau_n(\theta)\right\} \; ; \tag{26}$$

$$\pi_n(\theta) = \frac{P_n^{(1)}[\cos\theta]}{\sin\theta} \; , \quad \tau_n(\theta) = \frac{dP_n^{(1)}[\cos\theta]}{d\theta} \; , \tag{27}$$

where $P_n^{(m)}(\xi)$ is the associated Legendre polynomial of the first kind of degree n and order m.

Integration according to (24) with $\mathbf{M}_n$ and $\mathbf{N}_n$ given by (25),(26) and $d\Omega = \sin\theta d\theta d\phi$ can be performed directly (see Appendix 6 for details of calculation of particular integrals), and the result is

$$\int |\mathbf{E}_s(\mathbf{r})|^2 \, d\Omega =$$

$$2\pi|E_0|^2 \sum_{n=1}^{\infty}(2n+1)\left\{|c_n|^2 j_n^2(k_1 r) + |d_n|^2\left[\left(\frac{j_n(k_1 r)}{k_1 r}\right)^2 + \left(\frac{j_n(k_1 r)}{k_1 r} + j_n'(k_1 r)\right)^2\right]\right\} \; . \tag{28}$$

Further calculations require specifying the form of $\langle\rho(r)\rangle$. Below, we consider two cases: fractal distribution of the inclusion density and homogeneous distribution.

4. Fractal geometry of inclusions

An important characteristic of fractal clusters is the density-density correlation function, $\langle\rho(\mathbf{r}')\rho(\mathbf{r})\rangle$, which is proportional to $|\mathbf{r}' - \mathbf{r}|^{D-3}$ in the so-called intermediate asymptote region $R_0 \ll |\mathbf{r}' - \mathbf{r}| \ll R_c$, where D is the fractal dimension, R_0 is the minimum resolution scale and R_c is the characteristic size of the object (for example, the gyration radius R_g). If we set $\mathbf{r}' = 0$, the same scaling behavior should be true for the average density function, $\langle\rho(r)\rangle$, measured from the center of symmetry: $\langle\rho(r)\rangle \propto r^{D-3}$. For trivial objects, $D = 3$ and there is no long-range correlation in the system. For fractal clusters, D is, generally, less than 3. Specifically, for soot clusters $D \approx 1.8$[6]. The above scaling behavior of the density-density correlation function is only approximate. A number of studies[50,25], based on numerical simulations, showed that D itself can depend on $|\mathbf{r}' - \mathbf{r}|/R_c$. This phenomenon is known as multiscaling. However, the effects of multiscaling are, typically, small.

For our simplified consideration, we assume that D is a constant satisfying $1 \le D \le 3$. The case $D = 1$ corresponds to inclusions in the form of long linear sticks, while the case $D = 3$ corresponds to a homogeneous distribution of inclusions. If $D = 3$ (trivial geometry), the problem becomes mathematicaly equivalent to the Mie problem for a homogeneous dielectric sphere with some effective dielectric constant ϵ_{eff}. A nonperturbative analytic solution can be obtained in this case. However, this method has certain difficulties. First, the form of ϵ_{eff} is not obvious. For carbon inclusions of spherical shape and small concentration, one can use $\epsilon_{eff} = \epsilon_1 + (3v/V)(\epsilon_2 - \epsilon_1)/(\epsilon_2 + 2\epsilon_1)$[51]. But this formula is not applicable when the inclusions are not of spherical shape or form clusters of touching particles. An approach based on determining the effective dielectric function was used by Chowdhury et al.[35,40] who suggested averaging of the ϵ with the weight that includes the local intensity of the *unperturbed* electric field inside the sphere. Chowdhury et al. define two different averaged dielectric constants, one of which is used for computation of the internal (or external) field coefficients and the other - for the effective absorption (or gain). This method is somewhat similar to the perturbative approach used here in that it uses the unperturbed electric field to compute the effective ϵ. Different effective medium approximation were also used by Videen and Chylek[43]. The second difficulty is that the extinction and scattering cross sections in the analytical Mie solution are expressed as infinite series involving the scattering coefficient a_n, c_n; the absorption cross section must be calculated as the difference between these two values. When absorption is small, such calculation involves a numerical procedure of finding small difference between

two large numbers, and the round-off errors become very significant. Also, the direct Mie calculations in the case of a complex ϵ_{eff} involve spherical Bessel functions of a complex argument, which further complicates numerical procedures. Instead of finding an analytical solution based on some definition of ϵ_{eff}, we use in this paper the perturbative approach developed above for the $D = 3$ case. This approach is also valid for $D < 3$ (fractal geometry), when analytical solution can not be obtained, thus allowing us to maintain self-consistency of results.

An important question is how the fractal inclusions are located inside the microdroplets. This can be influenced by many factors such as chemical composition of soot particles, surface tension forces, temperature, etc. Formation of agglomerates of soot clusters and water can change the geometrical properties of the clusters due to the action of surface tension forces[52,53]. All these factors should be taken into account in further investigation. As was already discussed, the average density of inclusions must be spherically symmetrical if there is no distinguished direction in space. We also assume that, in accordance with the fractal density distribution, it obeys a power law with the scaling parameter D according to

$$\langle\rho(r)\rangle = \frac{vD}{4\pi a^D} r^{D-3} \text{ if } r < a \ . \tag{29}$$

Here the radius of the microdroplet, a, serves as the cut-off, and the density function (29) satisfies the normalization (3). Note that the validity of approximations developed above does not depend on the relation between a and λ.

Note that, according to its physical meaning as the probability to find a spot at the distance r from the droplet center occupied by carbon, $\langle\rho(r)\rangle$ cannot be greater than unity. In fact, the perturbation expansion used above relies on the assumption that $\langle\rho(r)\rangle \ll 1$. Formula (29) may seem to contradict this assumption when $r \to 0$. However, the divergence of $\langle\rho(r)\rangle$ at small r is not significant since all the physically important radial integrals converge fast enough at this limit (see below); thus the actual value of $\langle\rho(0)\rangle$ is not important. The small parameter of the perturbation expansion is v which is obviously present in the definition (29).

We will be interested in the numerical value of the absorption enhancement parameter G and its dependence of the fractal dimension D. When $D = 3$, the density of inclusions is homogeneous inside the water droplets, while when $D < 3$, it decreases from the center to the surface.

By using the average density function (29) and the result of angular integration of $|\mathbf{E}_s(\mathbf{r})|^2$ (28), one can express the absorption enhancement factor (16) in terms of simple radial integrals involving spherical Bessel functions. Inserting expressions (28),(29) into (16) and taking the integrals containing derivatives of spherical Bessel functions by parts, we arrive, after some rearrangement of terms, at the following result:

$$G = \frac{D}{2(k_1 a)^D} \sum_{n=1}^{\infty} (2n+1) \left\{ |c_n|^2 I_n(1) + |d_n|^2 \left[\frac{5-D}{2} x_1^{D-2} j_n^2(x_1) + \right. \right.$$

$$x_1^{D-1} j_n'(x_1) j_n(x_1) + I_n(1) + \left. \left. \left(4 - D + \frac{(2-D)(3-D)}{2} - n(n+1) \right) I_n(3) \right] \right\} \ , \tag{30}$$

$$I_n(\alpha) = \int_0^{x_1} x^{D-\alpha} j_n^2(x) dx \ . \tag{31}$$

The integrals $I_n(\alpha)$ converge for all physically interesting values of parameters (as discussed above) at both limits and must be evaluated numerically.

5. Numerical calculations

As was pointed out by Bohren and Huffmen[49], the diffraction parameter $x = ka$ (or $x_1 = \sqrt{\epsilon}x$) cannot be, in general, viewed as the only independent variable of the problem, although it may seem so from the mathematical form of equations (15) and (30). Indeed, when ϵ_1 depends on λ, $x_1/x \neq$ const. Instead, there are two physically independent parameters that define completely solution to the scattering problem, a and λ. However, when ϵ_1 does not depend on λ, $x_1/x = \epsilon_1 =$ const, and the diffraction parameter x becomes the only independent variable. Note that, in this case, we do not need to know whether x changes due to a change in a or in λ.

For the particular case of water, the assumption $x_1/x = $ const is a good approximation in the spectral range from 0.3μm to 2.0μm. For the constant room temperature $T = 20°C$ and pressure $P = 1$atm, ϵ_1 is accurately approximated in the spectral region 0.182μm $< \lambda < 2.770\mu$m by the following expression[54]:

$$\epsilon_1 = \frac{a_1}{\lambda^2 - \lambda_a^2} + a_2 + a_3\lambda^2 + a_4\lambda^4 + a_5\lambda^6 \ , \tag{32}$$

$$\lambda_a = 0.134\mu\text{m} \ ,$$

$$a_1 = 5.743 \cdot 10^{-3} \ , \ a_2 = 1.769 \ , \ a_3 = -2.797 \cdot 10^{-2} \ , \ a_4 = 8.715 \cdot 10^{-3} \ , \ a_5 = -1.414 \cdot 10^{-3} \ .$$

The imaginary part of the refractive index of water is very small in the optical spectral range, and following other authors (see, for example, Refs. 4, 41–43), we set it to zero. The spectral dependence of the refractive index of water, $\sqrt{\epsilon_1}$, is illustrated in Fig. 1. We have set $\sqrt{\epsilon_1} = 1.33 = $ const which allowed us to perform numerical calculation of the enhancement factor G as a function of one independent variable, $x = ka$. We allowed x to change from 0 to 1000. This range of x includes most of the practical values of a and λ. Thus, for $\lambda = 0.4\mu$m, a can vary from 0 to $\approx 60\mu$m.
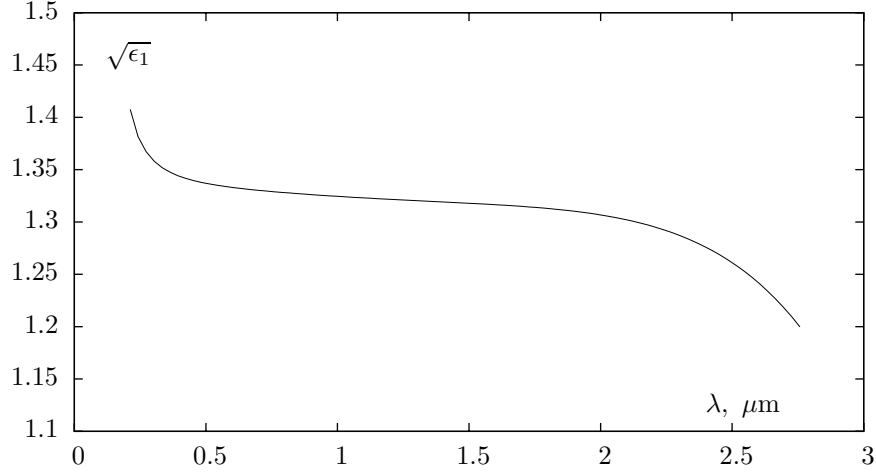

Fig. 1.   Refraction index $\sqrt{\epsilon_1}$ of water as a function of the wavelength λ (analytical approximation).

Now we turn to calculation of the internal field coefficients, c_n and d_n. We calculated the Bessel functions and their first derivatives that are used in the definitions (18) and (19) of the internal field coefficients, using the three-point recursion relation[55]:

$$j_{n+1}(\xi) = \frac{2n + 1}{\xi} j_n(\xi) - j_{n-1}(\xi) \ , \tag{33}$$

$$(2n + 1)j_n'(\xi) = nj_{n-1}(\xi) - (n + 1)j_{n+1}(\xi) \ . \tag{34}$$

The same recursion relations are valid for the spherical Hankel functions. Since we calculated the spherical functions of only real arguments, the numerical stability of the recursions was good, and the round-off errors were well within the required limits.

It is well known that the VSH maximum order n that gives significant contribution to the optical cross sections can be roughly estimated[49] as $n_{max} \approx x = ka$. The internal field coefficients $|c_n|^2$ and $|d_n|^2$ decrease dramatically for $n > n_{max}$, as illustrated in Fig. 2. In Fig. 2a, we plot the internal field coefficients for $\sqrt{\epsilon_1} = 1.33$ and $x = 259.664$. The specific value of x was chosen from the condition that the absorption cross-section has a resonance. In terms of VSH's, the resonance occurs for the order $n = 131$, when $|c_n|^2$ reaches the value of $\approx 3.23 \cdot 10^7$; there is also a big

10

number of weaker resonances of $|c_n|^2$. (Note that $|d_n|^2$ has no resonances.) Since the total number of VSH's that contribute to the absorption is of the order of 300, and $|c_{131}|^2$ is more than 5 orders of magnitude larger than the average background, we can conclude that the resonant VSH gives the prevailing input to the optical cross sections. For comparison, we plot in Fig. 2b the internal field coefficients for the same refraction index, but for an off-resonant value of $x = 260.400$. Both pictures look very similar, apart from the resonance order $n = 131$ in Fig. 2a.

(a)

(b)
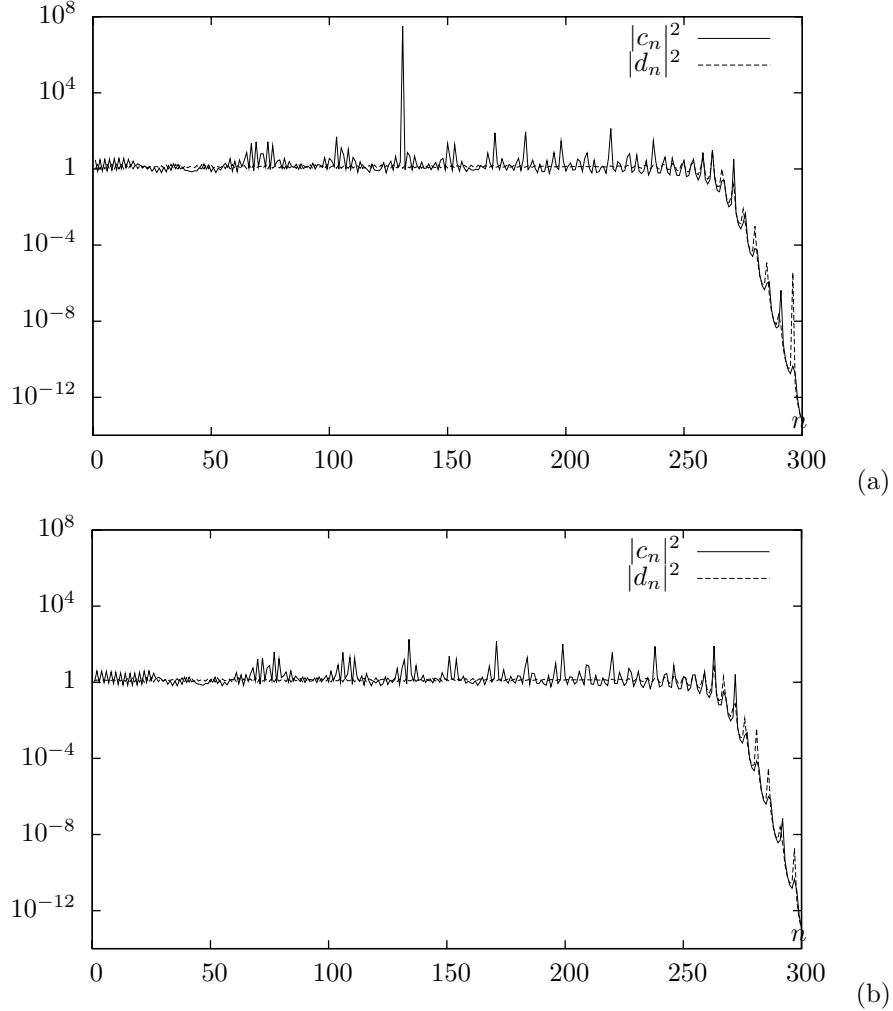
Fig. 2.   Internal field coefficients, $|c_n|^2$ and $|d_n|^2$, as functions of the VSH order, n. a) $x = 259.664$ (the resonance order $n = 131$); b) $x = 260.400$ (no pronounced resonances).

The numerical results for the absorption enhancement factor $G(x)$ are shown in Fig. 3 for $D = 1.1$ (Fig. 3a) and $D = 3.0$ (Fig. 3b). As can be seen in Fig. 3, $G(x)$ has a large number of quasi-random morphology-dependent resonances (due to the presence of resonances in internal field coefficients illustrated in Fig. 2), but only a very slight systematic dependence of $G(x)$ on x can be seen in the interval $10 < x < 1000$. The slight systematic increase of $G(x)$ can be attributed to an increase in average resonance quality with the size parameter x. It can be also seen from comparison of Figs. 3a and 3b that the enhancement factor is larger, on average, for $D = 1.1$ than for $D = 3.0$.

It is plausible to assume that in a polydisperse ensemble of microdroplets with size parameters in the wide range $10 < x < 1000$ the individual resonances are smoothed out and the average absorption enhancement factor, $\langle G \rangle$, which is practically important, is given by averaging of $G(x)$ over x. We performed such averaging in the interval of x specified above for different D ($1 \leq D \leq 3$) and the results are shown in Fig. 4. The averaging was performed with the step in x equal to 0.1. This step was small enough so that most resonances were visually resolved. Averaging

11

with a larger resolution resulted in a smaller value of $\langle G \rangle$ because the resonances in $G(x)$ are very narrow. It is important to emphasize the significance of the averaging process. For a randomly chosen x, $G(x)$ is, with a large probability, smaller than $\langle G \rangle$ by the factor of 4 or 5. Thus the resonances of $G(x)$ play an important role and should not be ignored. It should be noted that the averaging was performed in the region of $10 < x < 1000$ where there is no pronounced systematic dependence of $G(x)$ on x. For $x < 10$, the averaged G is considerably smaller.

(a)

(b)
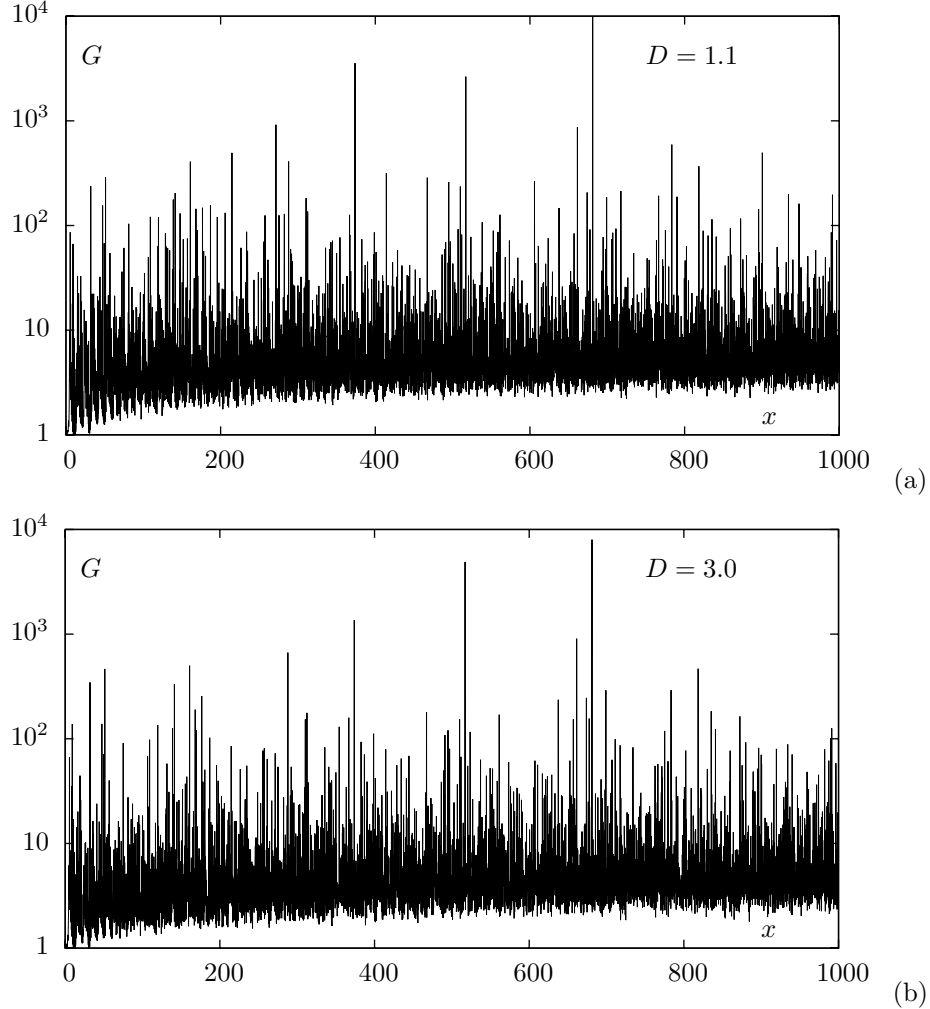
Fig. 3.   Absorption enhancement factor G as a function of the diffraction parameter $x = ka$ for different fractal dimensions D. a) $D = 1.1$; b) $D = 3.0$.

As can be seen in Fig. 4, $\langle G \rangle$ is maximum for $D = 1$ and decreases towards $D = 3$. For the practically important value $D = 1.8$, $\langle G \rangle \approx 16$, and the maximum variation of $\langle G \rangle$ with D does not exceed ± 6. The dependence of $\langle G \rangle$ on D can be explained by an interference between the fractal density function $\langle \rho(r) \rangle$ and the modes of a spherical resonator. It was shown by Berry and Percival that such interference can result in a significant increase of the scattering cross section for plane waves scattered by fractal clusters[16]. However, the absorption cross section was shown[16] to be independent of the fractal geometry (and, in fact, of any possible rearrangement of particles) in the case of the plane waves scattering. Consequently, in absorption, there is no positive interference between the fractal density function and plane waves. This follows from the simple fact that the amplitude of a plane wave is constant in space. Our results demonstrate that, for highly inhomogeneous modes of a spherical resonator, such interference can be significant for the absorption as well, resulting, in particular, in a stronger enhancement of absorption for the fractal distribution of inclusions than for the trivial one.
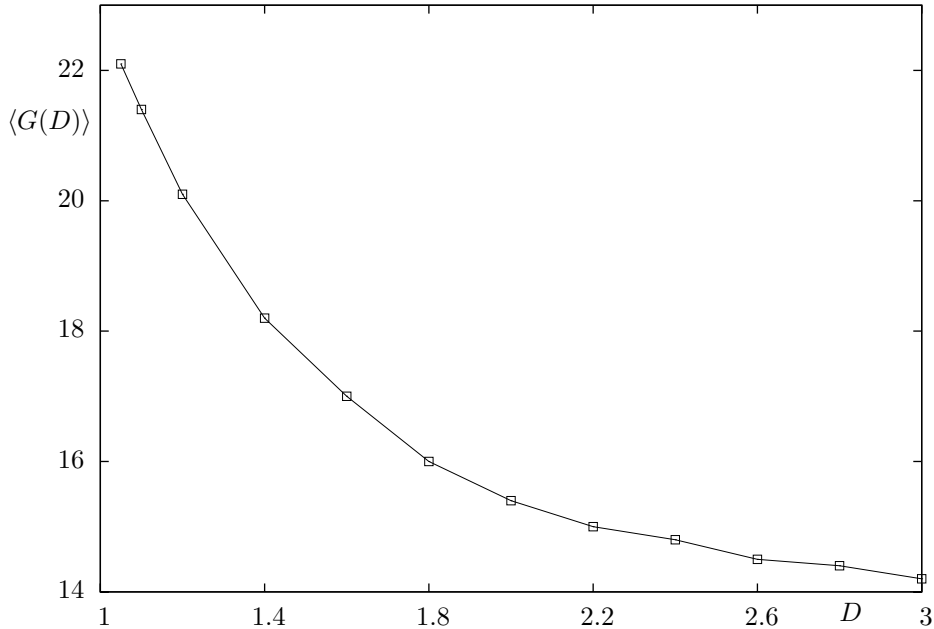
Fig. 4.   Average absorption enhancement factor $\langle G \rangle$ as a function of the fractal dimension, D.

6. Summary

As the main result of this paper, we calculated the average absorption enhancement factor for carbon soot clusters placed inside water droplets, compared to free soot clusters, as a function of the fractal dimension D. Both fractal and trivial (homogeneous) geometries of carbon inclusions were considered in a uniform way. We found that, in both cases, absorption is significantly increased when soot is placed inside water droplets. This is explained by the fact that spherical water droplets act like high-quality optical resonators and the intensity of electromagnetic fields inside the droplets can be much larger than that of an incident wave. From the point of view of the geometrical optics, the increase in absorption can be explained by the fact that light rays travel many times inside a spherical droplet reflecting from its boundary, and are absorbed by the inclusions during each pass (the total number of passes of a ray is roughly equal to the resonance quality). The absorption factor is larger for smaller fractal dimension of carbon inclusions, and changes from $\langle G \rangle \approx 14$ for $D = 3$ to $\langle G \rangle \approx 22$ for $D = 1$.

The enhancement factor G, defined as the ratio of the absorption cross sections of a soot cluster inside a water droplet to that in vacuum (or, more generally, in any transparent medium with refractive index close to unity, such as the atmosphere) shows no pronounced systematic dependence on the diffraction parameter $x = 2\pi a/\lambda$ for $10 < x < 1000$, where a is the droplet radius, apart from strong modulations associated with morphology-dependent resonances of the sphere which are smoothed out for an ensemble of droplets with different radiuses. This smoothing, or averaging, is essential for numerical estimate of the absorption enhancement. The averaging must be performed with a sufficiently high resolution in x in order to resolve all the morphology-dependent resonances which are very narrow. The averaged value $\langle G \rangle$ is 4 to 5 times larger than the typical off-resonance value $G(x)$ (calculated for a non-resonant x). Thus, the input of these narrow resonances is significant and should not be disregarded. This explains why our estimates of the absorption enhancement are considerably larger than those based on calculations for isolated values of x (Refs. 4, 43).

In the conclusion, we note that within the framework of the first Born approximation that was used throughout the article, the absorption cross section of a free carbon soot cluster excited by a plane wave is proportional to the total volume of carbon and does not depend on the cluster's geometrical configuration. However, this is not the case when the cluster is excited by the inhomogeneous modes of a spherical resonator instead of plane waves. In this case, the absorption is stronger, on average, if the inclusions tend to concentrate in the spatial regions where the intensity

of local fields is higher.

Appendix: Calculation of angular integrals

In spherical coordinates, the element of solid angle is $d\Omega = d\phi \sin(\theta)d\theta$. Integration over ϕ according to (24) with the VSH's defined by (25),(26) poses no difficulty since the only types of integrals over ϕ are

$$\int_0^{2\pi} \cos^4 \phi d\phi = \int_0^{2\pi} \sin^4 \phi d\phi = \frac{3\pi}{4} \; ;$$

$$\int_0^{2\pi} \sin^2 \phi \cos^2 \phi d\phi = \frac{\pi}{4} \; ; \quad \int_0^{2\pi} \sin^2 \phi d\phi = \int_0^{2\pi} \cos^2 \phi d\phi = \pi \; .$$

After performing integration over ϕ, we find that

$$\int_0^{2\pi} \mathbf{M}_n^2 d\phi = \pi j_n^2(k_1 r) \left[\pi_n^2(\theta) + \tau_n^2(\theta) \right] \quad , \tag{A1}$$

$$\int_0^{2\pi} \mathbf{N}_n^2 d\phi = \pi \left\{ \left[n(n+1) \frac{j_n(k_1 r)}{k_1 r} \right]^2 \sin^2 \theta \pi_n^2(\theta) + \left[\frac{j_n(k_1 r)}{k_1 r} + j_n'(k_1 r) \right]^2 \left[\pi_n^2(\theta) + \tau_n^2(\theta) \right] \right\} \; . \tag{A2}$$

The angular functions that are left after integration over ϕ are $\sin^2 \theta \pi_n^2(\theta)$ and $\pi_n^2(\theta) + \tau_n^2(\theta)$, where $\pi_n(\theta)$ and $\tau_n(\theta)$ are defined by (27). In the integration (24), these functions must be multiplied by $\sin \theta d\theta$.

With the standard substitution $\cos \theta = \xi$, and using the expression $P_n^{(1)}(\xi) = \sqrt{1 - \xi^2} dP_n(\xi)/d\xi$ that relates the Legendre polynomials P_n to the associated Legendre polynomials of the first order $P_n^{(1)}$, we find for the first integral:

$$I_1 = \int_0^{\pi} \sin^2 \theta \pi_n^2(\theta) \sin \theta d\theta = \int_{-1}^{1} (1 - \xi^2) \frac{dP_n}{d\xi} dP_n \; . \tag{A3}$$

Performing integration by parts, we find that

$$I_1 = \int_{-1}^{1} P_n \left[2\xi \frac{dP_n}{d\xi} - (1 - \xi^2) \frac{d^2 P_n}{d\xi^2} \right] d\xi \; . \tag{A4}$$

Because the Legendre polynomials satisfy the differential equation

$$(1 - \xi^2) \frac{d^2 P_n}{d\xi^2} - 2\xi \frac{dP_n}{d\xi} + n(n+1) P_n = 0 \; , \tag{A5}$$

the expression in the square brackets in (A4) can be simplified and

$$I_1 = n(n+1) \int_{-1}^{1} P_n^2(\xi) d\xi \; . \tag{A6}$$

The integral $\int_{-1}^{1} P_n^2(\xi) d\xi$ is well-known (see, for example, Ref. 56, formula 2.17.14.10) and is equal to $2/(2n + 1)$. Finally, we find

$$I_1 = \frac{2n(n+1)}{2n+1} \; . \tag{A7}$$

Calculation of the angular integral of $\pi_n^2(\theta) + \tau_n^2(\theta)$ is more lengthy. Again, we use substitution $\cos\theta = \xi$ and find

$$I_2 = \int_0^\pi \left[\pi^2(\theta) + \tau^2(\theta)\right]\sin\theta d\theta = \int_{-1}^1 \left\{\left(\frac{dP_n}{d\xi}\right)^2 + \left[(1-\xi^2)\frac{d^2P_n}{d\xi^2} - \xi\frac{dP_n}{d\xi}\right]^2\right\} d\xi . \tag{A8}$$

Next we express the second derivative of P_n with the use of differential equation (A5) and obtain the following expression for I_2:

$$I_2 = \int_{-1}^1 \left[(\xi^2 + 1)\frac{dP_n}{d\xi}dP_n - 2n(n+1)\xi P_n dP_n + n^2(n+1)^2 P_n^2 d\xi\right] . \tag{A9}$$

The first term in (A9) can be integrated with the use of the equality

$$\int_{-1}^1 (\xi^2+1)\frac{dP_n}{d\xi}dP_n = -I_1 + 2\int_{-1}^1 \left(\frac{dP_n}{d\xi}\right)^2 d\xi , \tag{A10}$$

where the integral I_1 is defined by (A3), and its value was calculated above (formula (A7)). The second integral in (A10) can be found in tables (see Ref. 56 , formula 2.17.14.24)) and is equal to $n(n+1)$. Therefore,

$$\int_{-1}^1 (\xi^2+1)\frac{dP_n}{d\xi}dP_n = \frac{4n^2(n+1)}{2n+1} . \tag{A11}$$

The second term in (A9) is easily integrated by parts with the use of $\int_{-1}^1 P_n^2(\xi)d\xi = 2/(n+1)$ and is equal exactly to the value in the right-hand side of Eq. (A11) with the opposite sign. Therefore, the first and the second terms in (A9) cancel each other. The third term in (A9) is also proportional to $\int_{-1}^1 P_n^2(\xi)d\xi$, so that the final result for I_2 is:

$$I_2 = \frac{2n^2(n+1)^2}{2n+1} . \tag{A12}$$

Finally, for the angular integrals, we find

$$\int_0^{2\pi} \mathbf{M}_n^2 d\Omega = \frac{2\pi n^2(n+1)^2}{2n+1} j_n^2(k_1 r) , \tag{A13}$$

$$\int_0^{2\pi} \mathbf{N}_n^2 d\Omega = \frac{2\pi n^2(n+1)^2}{2n+1} \left\{\left[\frac{j_n(k_1 r)}{k_1 r}\right]^2 + \left[\frac{j_n(k_1 r)}{k_1 r} + j_n'(k_1 r)\right]^2\right\} . \tag{A14}$$

Substitution of these expressions into (24) results in (28).

---

  1. P. Chylek, V. Ramaswamy, and R. J. Cheng, "Effect of graphitic carbon on the albedo of clouds," J. Atmospheric Sci. **41,** 3076–3084 (1984).
  2. J. E. Penna, R. E. Dickinson, and C. A. O'Neil, "Effects of aerosol from biomass burning on the global radiation budget," Science **256,** 1432–? (1992).

3. P. Chylek and J. Wong, "Effect of absorbing aerosols on global radiation budget," Geophys. Res. Lett. **22,** 929–931 (1995).

4. P. Chylek, G. B. Lesins, G. Videen, J. G. D. Wong, R. G. Pinnick, D. Ngo, and J. D. Klett, "Black carbon and absorption of solar radiation by clouds," J. Geophys. Res. **101,** 23365–23371 (1996).

5. R. P. Turco, O. B. Toon, T. P. Ackerman, J. B. Pillack, and C. Sagan, "Nuclear winter: Global consequences of multiple nuclear explosions," Science **222,** 1283–? (1983).

6. S. R. Forrest and T. A. Witten, "Long-range correlations in smoke-particle aggregates," J. Phys. A **12,** L109–L117 (1979).

7. C. W. Bruce, T. F. Stromberg, K. P. Gurton, and J. B. Mozer, "Trans-spectral absorption and scattering of electromagnetic radiation by disel soot," Appl. Opt. **30,** 1537–1546 (1991).

8. N. Lu and C. M. Sorensen, "Depolarized light scattering from fractal soot aggregates," Phys. Rev. E **50,** 3109–3115 (1994).

9. J. Cai, N. Lu, and C. M. Sorensen, "Analysis of fractal cluster morphology parameters: structural coefficient and density autocorrelation function cutoff," J. Colloid Interface Sci. **171,** 470–473 (1995).

10. E. F. Mikhailov and S. S. Vlasenko, "The generation of fractal structures in gaseous phase," Physics-Uspekhi **165,** 253–271 (1995).

11. S. D. Andreev and E. F. Mikhailov, "Fractal systems and studies of atmospheric aerosols," Bulletin of the Russian Acad. Sci. **32,** 743–750 (1996).

12. R. E. Danielson, D. R. Moore, and H. C. Van Hulst, "The transfer of visible radiation through clouds," J. Atmospheric Sci. **26,** 1078–1087 (1969).

13. H. Grassl, "Albedo reduction and radiative heating of clouds by absorbing aerosol particles," Contrib. Atmos. Phys. **48,** 199–210 (1975).

14. S. Twomey, "Computations of the absorption of solar radiation in clouds," J. Atmospheric Sci. **33,** 1087–1091 (1976).

15. K. Y. Kondratyev, V. I. Binenko, and O. P. Petrenchuk, "Radiative properties of clouds influenced by a city," Izvestia Akademii Nauk (USSR)- Fizika Atmosfery i Okeana **17,** 122–127 (1981).

16. M. V. Berry and I. C. Percival, "Optics of fractal clusters such as smoke," Optica Acta **33,** 577–591 (1986).

17. J. E. Martin and A. J. Hurd, "Scattering from fractals," J. Appl. Cryst. **20,** 61–78 (1987).

18. V. M. Shalaev, R. Botet, and R. Jullien, "Resonant light scattering by fractal clusters," Phys. Rev. B **44,** 12216–12225 (1991).

19. N. G. Khlebtsov and A. G. Mel'nikov, "Depolarization of light scattered by fractal smoke clusters: an approximate anisotropic model," Opt. Spectrosc. (USSR) **79,** 656–661 (1995).

20. N. G. Khlebtsov, "Spectroturbidimetrical analysis of the correlation function of fractal clusters density," Colloid J. **58,** 100–108 (1996).

21. F. Sciortino, A. Belloni, and P. Tartaglia, "Irreversible difusion-limited cluster aggregation: The behavior of the scattered intensity," Phys. Rev. E **52,** 4068–4079 (1995).

22. D. Asnaghi, M. Carpiteti, M. Giglio, and A. Vailati, "Light scattering studies of aggregation phenomena," Physica A **213,** 148–158 (1995).

23. P. Aymard, D. Durand, T. Nicolai, and J. C. Gimel, "A study of the fractal structure of aggregates formed after heat-induced denaturation of β-lactoglobulin," In *Fractal frontiers*, M. M. Novak and T. G. Dewey, eds., pp. 11–22 (World Scientific, Singapore, 1997).

24. V. A. Markel, V. M. Shalaev, E. Y. Poliakov, and T. F. George, "Fluctuations of light scattered by fractal clusters," J. Opt. Soc. Am. A **14,** 60–69 (1997).

25. V. A. Markel, V. M. Shalaev, E. Y. Poliakov, and T. F. George, "Numerical studies of second- and fourth-order correlation functions in cluster-cluster aggregates in application to optical scattering," Phys. Rev. E **55,** 7313–7333 (1997).

26. H.-B. Lin, A. L. Huston, J. D. Eversole, A. J. Campillo, and P. Chylek, "Internal scattering effects on microdroplet resonant emission structure," Opt. Lett. **17,** 970–972 (1992).

27. P. Chylek, D. Ngo, and R. G. Pinnik, "Resonance structure of composite and slightly absorbing spheres," J. Opt. Soc. Am. A **9,** 775–780 (1992).

28. R. L. Armstrong, J.-G. Xie, T. E. Ruekgauer, J. Gu, and R. G. Pinnik, "Effects of submicrometer-sized particles on microdroplet lasing," Opt. Lett. **18,** 119–121 (1993).

29. J.-G. Xie, T. E. Ruekgauer, R. L. Armstrong, and R. G. Pinnik, "Suppression of stimulated Raman scattering from microdroplets by seeding with nanometer-sized latex particles," Opt. Lett. **18,** 340–342 (1993).

30. J. Gu, T. E. Ruekgauer, J.-G. Xie, and R. L. Armstrong, "Effect of particulate seeding on microdroplet angular scattering," Opt. Lett. **18,** 1293–1295 (1993).

31. D. Ngo and R. G. Pinnik, "Supression of scattering resonances in inhomogeneous microdroplets," J. Opt. Soc. Am. A **11,** 1352–1359 (1994).

32. M. Kerker, D. D. Cooke, H. Chew, and P. J. McNulty, "Light scattering by structured spheres," J. Opt. Soc. Am. **68,**

592–601 (1978).

33. F. Borghese, P. Denti, R. Saija, and O. I. Sindoni, "Optical properties of spheres containing a spherical eccentric inclusion," J. Opt. Soc. Am. A **9,** 1327–1335 (1992).

34. M. M. Mazumder, S. C. Hill, and P. W. Barber, "Morphology-dependent resonances in inhomogeneous spheres: comparison of the layered," J. Opt. Soc. Am. A **9,** 1844–1853 (1992).

35. D. Q. Chowdhury, S. C. Hill, and M. M. Mazumder, "Quality factors and effective-average modal gain or loss in inhomogeneous spherical resonators," IEEE J. Quantum Electron. **29,** 2553–2561 (1993).

36. F. Borghese, P. Denti, and R. Saija, "Optical properties of spheres containing several spherical inclusions," Appl. Opt. **33,** 484–493 (1994).

37. K. A. Fuller, "Morpology-dependent resonances in eccentrically stratified spheres," Opt. Lett. **19,** 1272–1274 (1994).

38. K. A. Fuller, "Scattering and absorption cross sections of compounded spheres. I. Theory for external aggregation," J. Opt. Soc. Am. A **11,** 3251–3260 (1994).

39. S. C. Hill, H. I. Saleheen, and K. A. Fuller, "Volume current method for modelling light scattering by inhomogeneously perturbed spheres," J. Opt. Soc. Am. A **12,** 905–915 (1995).

40. D. Q. Chowdhury, S. C. Hill, and M. M. Mazumder, "Absorptive bistability in a dielectric sphere," Opt. Comm. **131,** 343–346 (1996).

41. K. A. Fuller, "Scattering and absorption cross sections of compounded spheres. II. calculations for external aggregation," J. Opt. Soc. Am. A **12,** 881–892 (1995).

42. K. A. Fuller, "Scattering and absorption cross sections of compounded spheres. III. Spheres containing arbitrarily located spherical inhomogeneities," J. Opt. Soc. Am. A **12,** 893–904 (1995).

43. G. Videen and P. Chylek, "Scattering by a composite sphere with an absorbing inclusion and effective medium approximations," Opt. Comm. **158,** 1–6 (1998).

44. P. Chylek, private communication (unpublished).

45. H. C. Chen, *Theory of electromagnetic waves* (McGraw-Hill Book Co., New York, 1983).

46. J. A. Kong, *Theory of electromagnetic waves* (John Wiley & Sons, New York, 1975).

47. V. A. Markel, "Antisymmetrical optical states," J. Opt. Soc. Am. B **12,** 1783–1791 (1995).

48. V. A. Markel and E. Y. Poliakov, "Radiative relaxation time of quasi-normal optical modes in small dielectric particles," Phil. Mag. B **76,** 895–909 (1997).

49. C. F. Bohren and D. R. Huffman, *Absorption and scattering of light by small particles* (John Wiley & Sons, New York, 1983).

50. C. Amitrano, A. Coniglio, P. Meakin, and M. Zannetti, "Multiscaling in diffusion-limited aggregation," Phys. Rev. B **44,** 4974–4977 (1991).

51. L. D. Landau and L. P. Lifshitz, *Electrodynamics of continuous media* (Pergamon Press, Oxford, 1984).

52. E. F. Mikhailov, S. S. Vlasenko, T. I. Ryshkevitch, and A. A. Kiselev, "Soot structure investigation: Adsorbtional properties," J. Aerosol Sci. **27,** S709–S710 (1996), suppl. 1.

53. E. F. Mikhailov, S. S. Vlasenko, A. A. Kiselev, and T. I. Ryshkevich, "Modification of carbon cluster fractal structure due to capillary forces," In *Fractal frontiers*, M. M. Novak and T. G. Dewey, eds., pp. 393–402 (World Scientific, Singapore, 1997).

54. I. Thormahlen, J. Straub, and U. Grigull, "Refractive index of water and its dependence on wavelength, temperature and density," J. Phys. Chem. Ref. Data **14,** 933–945 (1985).

55. H. Bateman, *Higher transcendental functions* (McGraw-Hill Book Co., New York, 1953), Vol. 2.

56. A. P. Prudnikov, Y. A. Brychkov, and O. I. Marichev, *Integrals and series. Special functions* (Gordon and Breach Science Pub., New York, 1986), Vol. 2.